Turkish Journal of Electrical Engineering & Computer Sciences

http://journals.tubitak.gov.tr/elektrik/

Research Article

Turk J Elec Eng & Comp Sci
(2018) 26: 1724 – 1735

doi:10.3906/elk-1712-92

Simulation of infinite periodic graphene planar grating in the THz range by the method of singular integral equations

Mstislav KALIBERDA[1,*], **Leonid LYTVYNENKO**[2], **Sergey POGARSKY**[1]
[1]Department of Radiophysics, V. Karazin National University of Kharkiv, Kharkiv, Ukraine
[2]Institute of Radio Astronomy of the National Academy of Sciences of Ukraine, Kharkiv, Ukraine

Received: 06.12.2017 • **Accepted/Published Online:** 03.04.2018 • **Final Version:** 27.07.2018

Abstract: Plane wave diffraction by the infinite periodic planar graphene grating and infinite grating above a perfectly conducting plane in the THz range is considered. The mathematical model is based on the graphene surface impedance and the method of singular integral equations. A comparison with finite grating is made. Reflectance, transmittance, and absorbance are studied as a function of graphene and grating parameters.

Key words: Graphene strip, Kubo formalism, infinite periodic grating, singular integral equation, Nystrom-type algorithm

1. Introduction

In [1], diffraction by finite graphene grating was described with the use of the method of singular integral equations (SIEs). In this paper we are going to use this method to consider infinite periodic grating of graphene strips.

Graphene gratings may be used as frequency selective surfaces, sensors, plasmon waveguides, and in tunable antennas [2–6]. A review of the application of the finite element method, finite-difference time-domain method, and method of moments was presented in [7]. The method of integral equations was used for a free-standing graphene strip and disc in [8], and for a finite number of graphene strips in [9]. In [10,11], the Fourier expansion method was used for the graphene infinite periodic strip grating under normal incidence. Strict analysis of the same grating under arbitrary incidence with the use of the semiinverse procedure and the method of analytical regularization was given in [12]. In [13], the method proposed in [12] was developed for the infinite periodic graphene grating embedded in a dielectric slab.

Classical methods also can be applied to study periodic gratings of material strips such as the Riemann–Hilbert problem technique [14]. In [15], a theory of summation equations was developed. The method for solving summation equations with different kernels in the form of trigonometric functions, Mathieu and Bessel functions, adjoint Legendre functions, and Jacobi polynomials was proposed. An approach that deals with operators with singularities of stationary boundary value problems in theory of wave diffraction by periodic gratings was proposed in [16]. Here we propose a method that leads to Cauchy-type SIEs. These equations have similar forms for the infinite periodic gratings as well as for the finite gratings (only the kernel-function and right-hand side differ), so a unified method of numerical solution can be used. All these methods are equal in effectiveness and the use of one of them does not preclude the enforcement of others.

*Correspondence: kaliberdame@yandex.ua

In this paper, we consider H-polarized wave diffraction by the infinite periodic graphene grating placed in the free space and above a perfectly electric conducting (PEC) plane. The numerical scheme of the solutions of the obtained SIEs is based on the Nystrom-type method of discrete singularities and has guaranteed convergence [17–22]. Complex-valued graphene conductivity σ is obtained using Kubo formalism [23,24]. The graphene grating above a PEC plane with dipole excitation was used as an antenna with tunable direction pattern in [25].

We will obtain the solution of the problems in several steps. First, we represent a scattered field using the Fourier series with unknown amplitudes. After that, from boundary conditions, dual series equations will be presented. Then they will be reduced to the SIEs.

2. Statement of the problem

Consider two diffraction problems. The first is the H-polarized wave diffraction by the infinite periodic grating of graphene strips placed in the $z = 0$ plane. The second problem is diffraction by the infinite periodic graphene grating above the PEC plane. The infinite grating is described by the period l and strip width $2d$. The strips are infinite along the x-axis; the distance between the grating and PEC plane in the second problem is h. Let us place the coordinate system as is shown in Figures 1a and 1b.

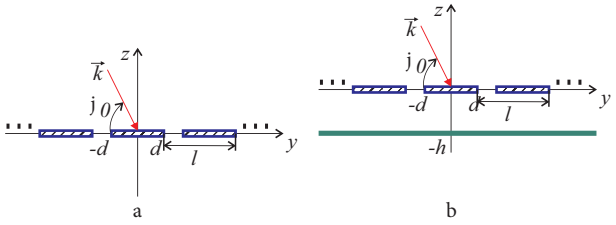

Figure 1. Structure geometry: a) free-standing graphene periodic grating, b) graphene periodic grating above PEC plane.

We seek the total field as a sum of the incident and scattered field. In the case of graphene strips, the following boundary conditions should be satisfied [8,9,26]:

$$\frac{1}{2}\left(E_y^+ + E_y^-\right) = \frac{1}{\sigma}\left(H_x^+ - H_x^-\right), \tag{1}$$

$$E_y^+ = E_y^-, \quad z = 0, \quad y \text{ outside the strips}, \tag{2}$$

and

$$E_y = -\frac{1}{i\omega\varepsilon_0}\frac{\partial H_x}{\partial z},$$

where ε_0 is the permittivity of free space. "+" corresponds to the field above the grating $(z \to +0)$ and "–" to the field below the grating $(z \to -0)$.

3. Infinite periodic grating

Let us consider infinite periodic grating of graphene strips placed in the $z = 0$ plane (see Figure 1a). The H-polarized field is incident on the grating from the half space $z > 0$:

$$H_x^i(y, z) = \exp\left(ik(\zeta_0 y - \gamma_0 z)\right),$$

where k is the wave number, in the general case $\zeta_n = \frac{2\pi n}{kl} + \sin\alpha$, $\gamma_n = \sqrt{1-\left(\frac{2\pi n}{kl}+\sin\alpha\right)^2}$, $Re\gamma_n \geq 0$, $Im\gamma_n \geq 0$, and $\phi_0 = \pi/2 - \alpha$ is the incidence angle to the y-axis. We seek the total field as a sum of the incident and scattered field. We represent the scattered field in the form of a Fourier series with unknown amplitudes a_n [14,21,22,27]:

$$H_x(y,z) = H_x^i(y,z) + sgn(z)\sum_{n=-\infty}^{\infty} a_n \exp\left(ik(\zeta_n y + \gamma_n|z|)\right), \quad z \neq 0.$$

The scattered field satisfies the Helmholtz equation outside the strips, the continuity condition of Eq. (2), and radiation and periodicity conditions. We suppose that the scattered field also satisfies the edge condition near the infinitely thin strips. Enforcement of the boundary conditions of Eqs. (1) and (2) leads to the dual series equations for a single period, $|y| < l/2$:

$$\sum_{n=-\infty}^{\infty} a_n \exp\left(i\frac{2\pi n}{l}y\right) = 0, \quad |y| \geq d \text{ (for slot)}, \tag{3}$$

$$\frac{2ik}{\sigma Z}\sum_{n=-\infty}^{\infty} a_n \exp\left(i\frac{2\pi n}{l}y\right) + \sum_{n=-\infty}^{\infty} a_n\gamma_n \exp\left(i\frac{2\pi n}{l}y\right) = \gamma_0, \quad |y| < d \text{ (for graphene strip)}. \tag{4}$$

Reduce Eqs. (3) and (4) to the SIEs with additional condition as was done in [21,27] for the PEC case. We present this technique brie?y here. Let us introduce dimensionless quantities $\xi = 2\pi y/l$, $\kappa = kl/(2\pi)$, $\delta = 2\pi d/l$. Using asymptotic behavior for $\gamma_n \sim i\frac{|n|}{\kappa} + O(1/|n|)$, when $n \to \infty$, represent it as a sum of vanishing and nonvanishing terms, $\gamma_n = \left(\gamma_n - i\frac{|n|}{\kappa}\right) + i\frac{|n|}{\kappa}$. Rewrite Eq. (4) as follows:

$$i\sum_{n=-\infty}^{\infty}\frac{|n|}{\kappa}a_n \exp(in\psi) + \frac{2ik}{\sigma Z}\sum_{n=-\infty}^{\infty} a_n \exp(in\psi) + \sum_{n=-\infty}^{\infty} a_n\left(\gamma_n - i\frac{|n|}{\kappa}\right)\exp(in\psi) = \gamma_0, \quad |\psi| < \delta.$$

Using the periodic Hilbert operator, $P_{2\pi}G(\psi) = \frac{1}{2\pi}PV\int_{-\pi}^{\pi} ctg\frac{\xi-\psi}{2}G(\xi)d\xi$, $P_{2\pi}\exp(in\psi) = isgn(n)\exp(in\psi)$, the nonvanishing term (first series) is transformed to the singular integral. Then the vanishing terms (second and third series) are collected to the kernel function. Here PV means the Cauchy principal value integral and $G(\xi)$ is an arbitrary function. Eq. (4) is transformed into a SIE:

$$\frac{1}{\pi}PV\int_{-\delta}^{\delta}\frac{F(\xi)}{\xi-\psi}d\xi + \frac{1}{\pi}\int_{-\delta}^{\delta}K(\psi,\xi)F(\xi)d\xi = i\kappa\gamma_0, \tag{5}$$

where

$$a_n = \frac{1}{2\pi in}\int_{-\delta}^{\delta}F(\xi)\exp(-in\xi)d\xi, \tag{6}$$

$$a_0 = -\frac{1}{\pi}\int_{-\delta}^{\delta}\frac{\xi}{2}F(\xi)d\xi. \tag{7}$$

The kernel function $K(\psi,\xi)$ is

$$K_{2\pi}(\psi,\xi) = -\frac{\kappa}{2}\sum_{\substack{n=-\infty\\ n\neq 0}}^{\infty}\left(\frac{i|n|}{\kappa}-\gamma_n\right)\frac{\exp\left(in(\psi-\xi)\right)}{n} + i\gamma_0\kappa\frac{\psi-\xi}{2} + \left(\frac{1}{\psi-\xi}-\frac{1}{2}\cot\left(\frac{\psi-\xi}{2}\right)\right) + q(\psi,\xi), \tag{8}$$

$$q(\psi,\xi) = \begin{cases} \frac{2i\kappa\pi}{\sigma Z}, & \xi \le \psi, \\ 0, & \xi > \psi. \end{cases}$$

Since the series in Eq. (8) converges and function $\left(\frac{1}{\psi-\xi}-\frac{1}{2}\cot\left(\frac{\psi-\xi}{2}\right)\right)$ has finite limit, when $\psi\to\xi$, the kernel function $K(\psi,\xi)$ is the regular one for all ψ and $\xi\in(-\pi;\pi)$. The appropriate choice of discretization scheme in the method of discrete singularities provides that $\frac{\psi-\xi}{2}\neq\pm\pi$. Numerical study (see Figure 2) shows that no difficulties with the stability of the numerical solution are observed when the strip width approaches the value of the period, $2d\to l$, and $\frac{\psi-\xi}{2}\to\pm\pi$.

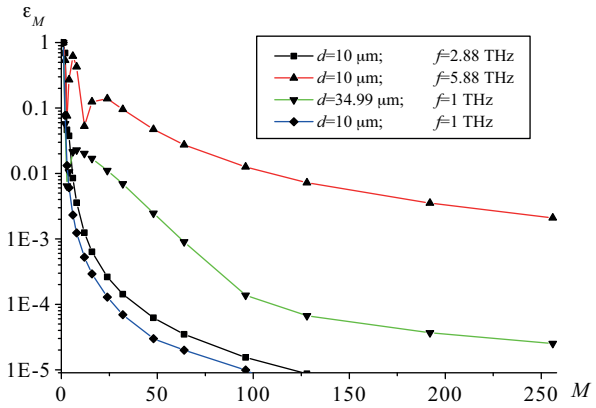

Figure 2. Relative error ε_M vs. number of nodes, $d=10\ \mu m$, $f=2.88$ THz (black curve); $d=10\ \mu m$, $f=5.88$ THz (red curve); $d=34.99\ \mu m$, $f=1$ THz (green curve); $d=10\ \mu m$, $f=1$ THz (blue curve); $l=70\ \mu m$, $\phi_0=90^0$, $\tau=1$ ps, $T=300$ K, $\mu_c=0.5$ eV.

Eq. (3) give rise to additional conditions, which provides the unique solution of Eq. (5):

$$\frac{1}{\pi}\int_{-\delta}^{\delta}F(\xi)d\xi = 0. \tag{9}$$

4. Infinite periodic grating above perfectly electric conducting plane

In the case of the structure represented in Figure 1b, we seek the total field as follows:

$$H_x(y,z) = \exp\left(ik(\zeta_0 y-\gamma_0(z+h))\right) + \exp\left(ik(\zeta_0 y+\gamma_0(z+h))\right) + H^{\pm}(y,z), \tag{10}$$

where $\exp\left(ik(\zeta_0 y-\gamma_0(z+h))\right)$ is an incident field, $\exp\left(ik(\zeta_0 y+\gamma_0(z+h))\right)$ is a field reflected by the PEC plane, $H^{\pm}(y,z)$ is a field scattered by the grating, "+" corresponds to the field above the grating, $z>0$, and

"–" corresponds to the field under the grating, $-h < z < 0$. Scattering by the grating field may be represented as follows:

$$H^{+}(y,z) = \sum_{n=-\infty}^{\infty} c_n \exp\left(ik(\zeta_n y + \gamma_n z)\right), \quad z > 0,$$

$$H^{-}(y,z) = -i \sum_{n=-\infty}^{\infty} c_n \frac{\cos\left(k\gamma_n(z+h)\right)}{\sin\left(\gamma_n kh\right)} \exp\left(ik\zeta_n y\right), -h < z < 0, \tag{11}$$

where c_n are unknown amplitudes. In Eqs, (10) and (11) we take into account the boundary conditions on the PEC plane. Using Eqs. (1) and (2), dual series equations may be obtained for a single period:

$$\sum_{n=-\infty}^{\infty} c_n \left(1 + i\cot(\gamma_n kh)\right) \exp\left(ik\zeta_n y\right) = 0, \quad |y| \geq d \text{ (for slot)}, \tag{12}$$

$$\frac{ik}{\sigma Z_0} \sum_{n=-\infty}^{\infty} c_n \left(1 + i\cot(\gamma_n kh)\right) \exp\left(ik\zeta_n y\right) + ik \sum_{n=-\infty}^{\infty} \gamma_n C_n \exp\left(ik\zeta_n y\right) = 2k\gamma_0 \sin\left(\gamma_0 kh\right) \exp(ik\zeta_0 y), |y| < d$$

(for graphene strip). $|y| < d$ (13)

To reduce Eqs. (12) and (13) to the SIEs, introduce the following function:

$$D_n = c_n \left(1 + i\cot(\gamma_n kh)\right),$$

and introduce dimensionless quantities. Then Eqs. (13) and (13) are

$$\sum_{n=-\infty}^{\infty} D_n \exp\left(iny\right) = 0, \quad |y| \geq d \text{ (for slot)},$$

$$\frac{2}{\sigma Z_0} \sum_{n=-\infty}^{\infty} D_n \exp\left(iny\right) + \sum_{n=-\infty}^{\infty} \frac{2\gamma_n}{1 + i\cot\left(\gamma_n kh\right)} D_n \exp\left(iny\right) = -4i\gamma_0 \sin\left(\gamma_0 kh\right),$$

$|y| < d$ (for graphene strip).

Taking into account asymptotic behavior for $\frac{2\gamma_n}{1+i\cot(\gamma_n kh)} \sim i\frac{|n|}{\kappa} + O(1/|n|)$, when $n \to \infty$, as in Section 2 we may obtain SIEs with additional conditions in the form of Eqs. (5) and (9):

$$\frac{1}{\pi} PV \int_{-\delta}^{\delta} \frac{F(\xi)}{\xi - \psi} d\xi + \frac{1}{\pi} \int_{-\delta}^{\delta} K(\psi, \xi) F(\xi) d\xi = 4\kappa\gamma_0 \sin\left(\gamma_0 kh\right), \tag{14}$$

$$\frac{1}{\pi} \int_{-\delta}^{\delta} F(\xi) d\xi = 0.$$

To obtain the expression for the kernel function and for coefficients D_n we may substitute $\frac{2\gamma_n}{1+i\cot(\gamma_n kh)}$ instead of γ_n in Eq. (8) and substitute D_n instead of a_n in Eqs. (6) and (7):

$$K_{2\pi}(\psi,\xi) = -\frac{\kappa}{2}\sum_{\substack{n=-\infty\\ n\neq 0}}^{\infty}\left(\frac{i|n|}{\kappa}-\frac{2\gamma_n}{1+i\cot(\gamma_n kh)}\right)\frac{\exp(in(\psi-\xi))}{n}$$

$$+\frac{i\kappa\gamma_0}{1+i\cot(\gamma_0 kh)}\frac{\psi-\xi}{2}+\left(\frac{1}{\psi-\xi}-\frac{1}{2}\cot\left(\frac{\psi-\xi}{2}\right)\right)+q(\psi,\xi),$$

$$D_n = \frac{1}{2\pi i n}\int_{-\delta}^{\delta}F(\xi)\exp(-in\xi)d\xi, \quad n\neq 0,$$

$$D_0 = -\frac{1}{\pi}\int_{-\delta}^{\delta}\frac{\xi}{2}F(\xi)d\xi.$$

Solution of Eqs. (5), (9), and (14) may be obtained by the method of discrete singularities [17–20].

5. Numerical results

Denote reflection, transmission, and absorbance coefficients as R, T, and A. They correspond to the power of the reflected field, the power of the transmitted field, and the absorbed power of the incident field. We use such graphene parameters as relaxation time τ, chemical potential μ_c, and temperature T.

5.1. Validation of results: infinite periodic grating

The convergence of the method was highlighted in many works (see, for example, [1,19,22,26,28]). The method of the solution provides the algebraic convergence with increasing matrix dimension. We can introduce the relative error of the reflection coefficient as follows:

$$\varepsilon_M = |T(R)-T(2R)|\,/\,|T(2R)|\,,$$

where M is the number of nodes in the quadrature rule or dimension of the matrix after discretization of Eqs. (5) and (9) by the method of discrete singularities. The dependences of ε_M vs. M are represented in Figure 2. The values of parameters are taken as follows: two curves are plotted near the first ($f = 2.88$ THz) and second ($f = 5.88$ THz) plasmon resonance; to check the stability of the algorithm when $\frac{\psi-\xi}{2}\to\pm\pi$ we take strip width as almost equal to the period, $d = 34.99\ \mu m$; for comparison one curve is also plotted for the value of frequency $f = 1$ THz. As one can see, the number of interpolation nodes that one should take is mainly defined by the value of the normalized strip width kd: with the parameter kd increasing, the number of nodes should also be increased.

To validate the results for the infinite periodic grating we compare them with results for the finite grating. Here we use the methodology that was successfully proposed in [9]. Suppose that the field scattered by the finite grating is expressed via a Fourier integral with known spectral function $C(\xi)$ [1]:

$$H_x^s(y,z) = sgn(z)\int_{-\infty}^{\infty}C(\xi)\exp(ik\xi y+ik\gamma(\xi)|z|)d\xi,$$

where $\gamma(\xi) = \sqrt{1-\xi^2}$, $Re\gamma \geq 0$, and $Im\gamma \geq 0$. Then the transmission, reflection, and absorption coefficients of the finite grating of N strips may be written as follows [9]:

$$T_N = 1 + \frac{\pi\zeta}{kdN\sin\phi_0}\int_0^{\pi}\left(C(-\cos(\phi))\sin\phi\right)^2 d\phi - Re\left(C(\cos\phi_0)\right),$$

$$R_N = \frac{\pi\zeta}{kdN\sin\phi_0}\int_0^{\pi}\left(C(-\cos(\phi))\sin\phi\right)^2 d\phi,$$

$$A_N = 1 - T_N - R_N,$$

where $\zeta = 2d/l$. The relative deviation may be expressed as:

$$\delta_T = \left|T_N - T\right| / \left|T\right|.$$

The results are presented in Figure 3. The results correlate well with each other. As was reported in [9], the difference is observed near the Rayleigh anomalies (zoomed in on in Figure 3a). As an example, Figure 3b represents relative deviation only for the transmission coefficient.

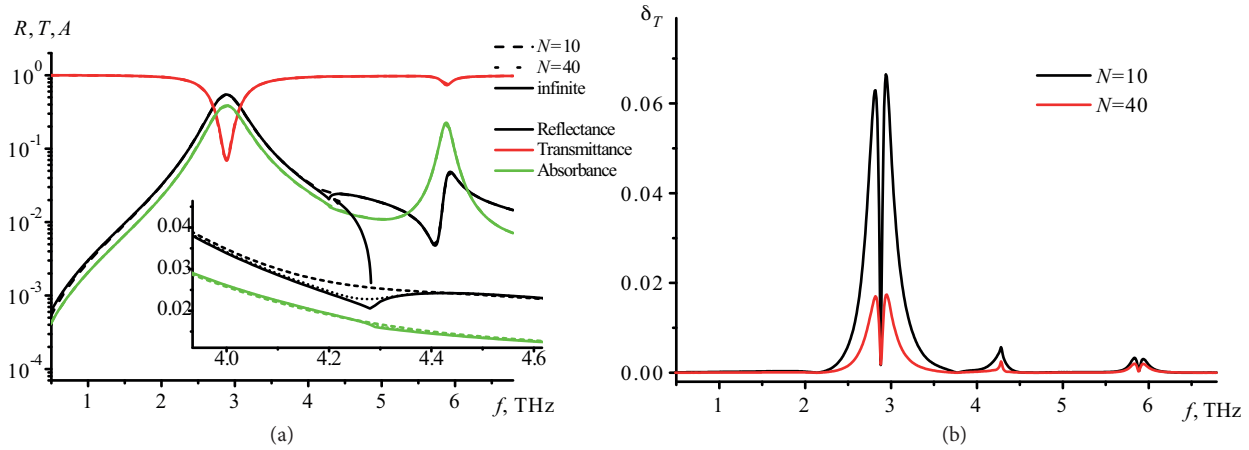

Figure 3. Comparison with finite grating, $d = 10\ \mu m$, $l = 70\ \mu m$, $\phi_0 = 90^0$, $\tau = 1$ ps, $T = 300$ K, $\mu_c = 0.5$ eV. a) Dependences of reflection (black curves), transmission (red curves) and absorbance (green curves) vs. frequency for finite gratings of $N = 10$ strips (dashed curves), $N = 40$ strips (dotted curves) and infinite grating (solid curves); b) dependences of $\delta_T(f)$ vs. frequency.

5.2. Validation of results: infinite periodic grating above a perfectly electric conducting plane

To validate results for the infinite periodic grating above the PEC plane in the case when only one fundamental plane wave can propagate, $kl << 2\pi$, $\phi_0 = 90^0$, we use complex reflection $r = a_0$ and transmission $t = 1 - a_0$ coefficients of the infinite grating. Taking into account that $t = 1 - r$, one may obtain relations between Fourier amplitudes of the reflected field C and field between the grating and the plane D and E (see Figure 4 for notations):

$$C = r + teD = r + eD - reD, \tag{15}$$

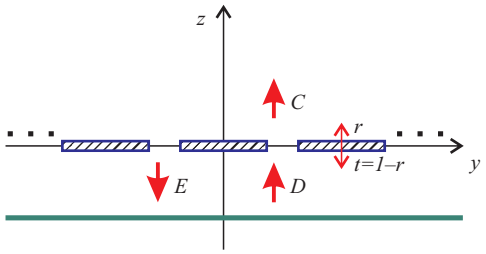

Figure 4. Notations for the periodic grating above the PEC plane.

$$E = t + reD = 1 - r + reD, \tag{16}$$

$$D = eE, \tag{17}$$

where $e = \exp(ikh)$. Figure 5 shows plots for the reflected power obtained from Eq. (14) (asterisks) and from the rigorous solution of Eq. (13). Good agreement is observed up to $kh = 2\pi$ when ± 1 plane waves are excited and scalar Eqs. (15), (16), and (17) are not valid.

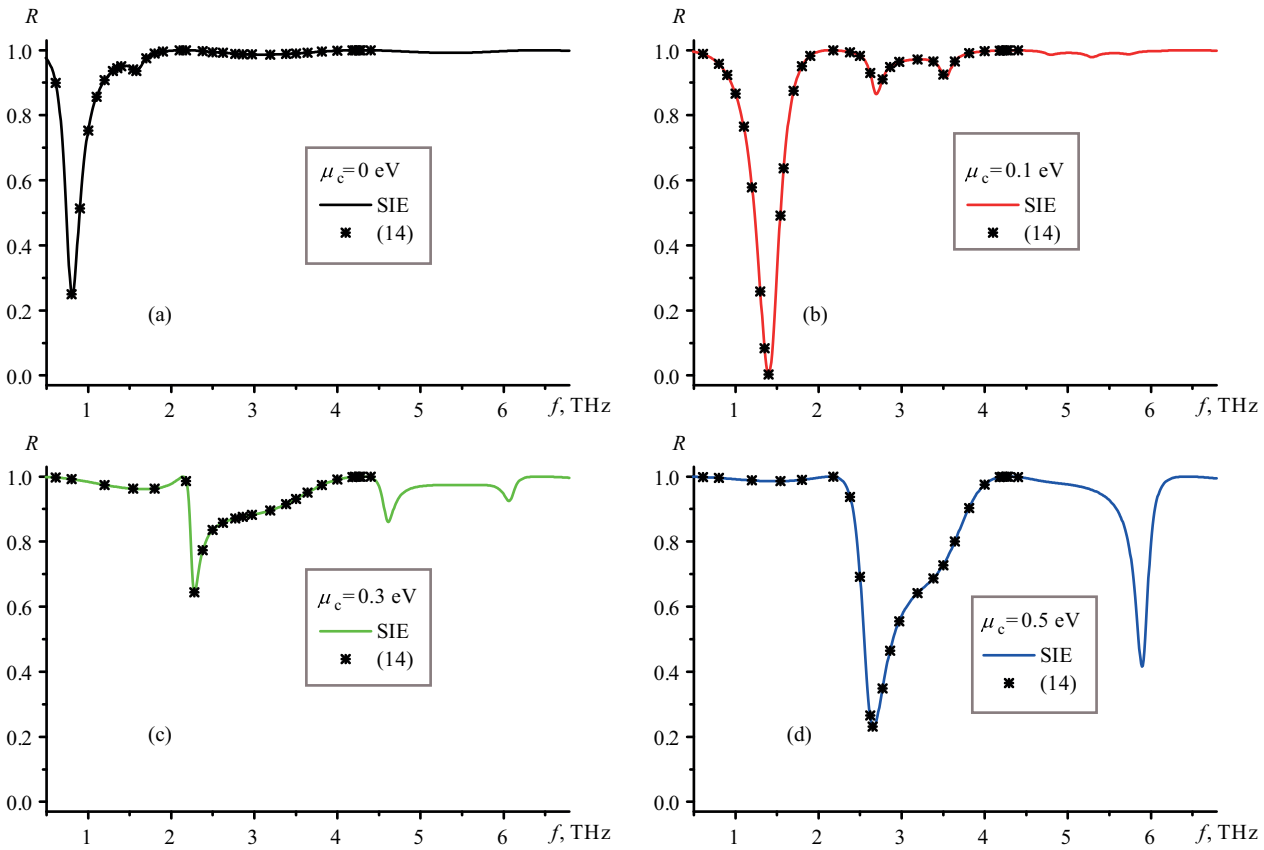

Figure 5. Dependences of reflection vs. frequency for infinite gratings above the PEC plane, $d = 10\ \mu m$, $l = 70\ \mu m$, $h = 70\ \mu m$, $\phi_0 = 90^0$, $\tau = 1$ ps, $T = 300$ K. (a) $\mu_c = 0$ eV; (b) $\mu_c = 0.1$ eV; (c) $\mu_c = 0.3$ eV; (d) $\mu_c = 0.5$ eV. Solution of SIE (solid line) and solution of Eq. (14) (asterisks).

5.3. Numerical analysis

Figure 6 shows dependences of the reflection, transmission, and absorbance coefficients vs. frequency of the infinite periodic grating for different values of chemical potential μ_c. With chemical potential increasing, the resonances shift to the greater values of frequency. The reflectance near plasmon resonances becomes more pronounced. A different situation is observed if one places the PEC plane below the grating (see Figure 5 or Figure 7). Figures 7a–7d show the results of calculations for the infinite grating above the PEC plane for different values of chemical potential μ_c and distance between the grating and the plane h. Since $A = 1 - R$, we represent only reflected power. In the case of the single grating one may observe a significant increase in absorbance near plasmon resonances. In the case of the grating above the plane there are such values of distance h that absorbance is almost absent over the whole considered frequency range including bands near plasmon resonances, where reflectance is almost 1, $R \approx 1$ (see Figure 7d, $h = 52\ \mu m$). However, for certain values of h and μ_c, almost total absorbance occurs, $A \approx 1$ (see Figures 7b and Figure 7c near the first plasmon resonance). Moreover, shifts in resonance frequencies are observed.

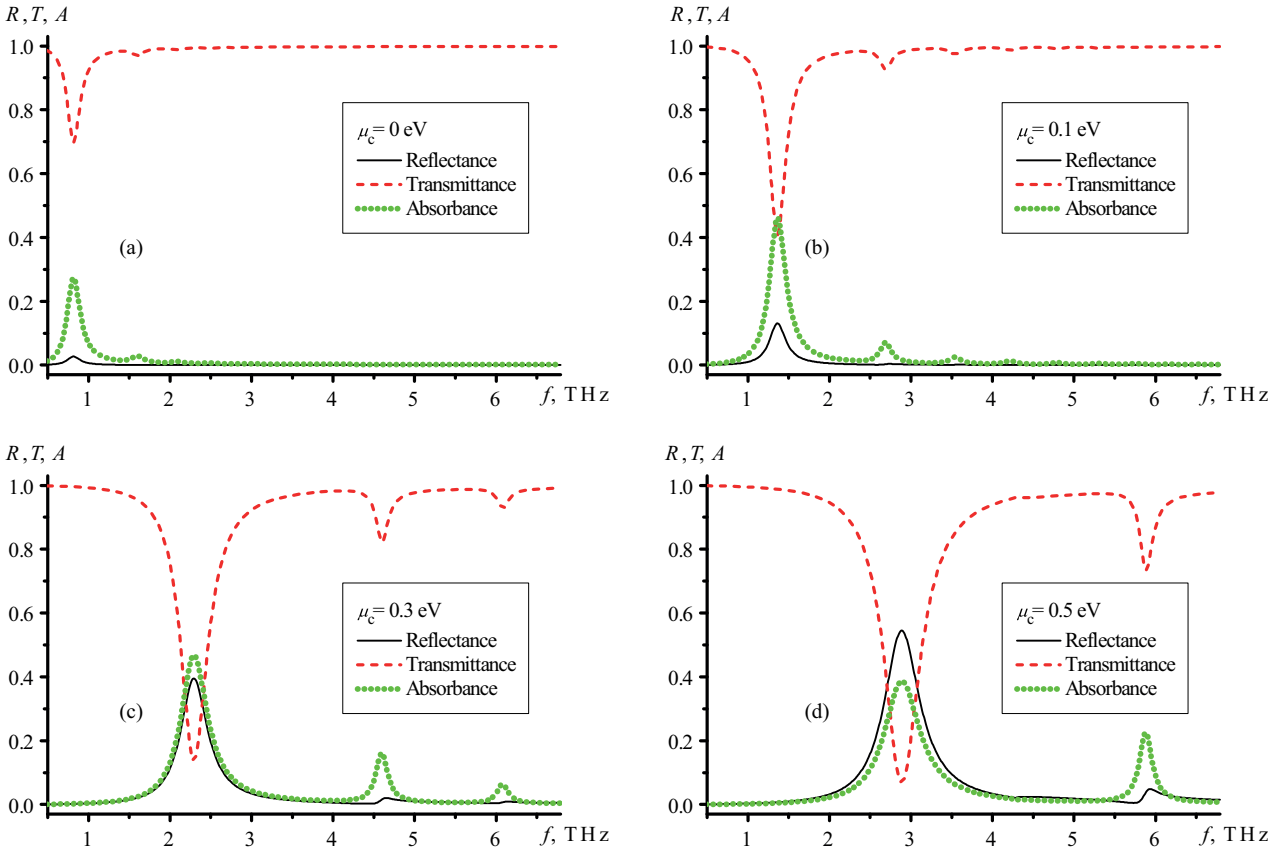

Figure 6. Dependences of reflection (solid curves), transmission (dashed curves), and absorbance (dotted curves) vs. frequency for infinite gratings, $d = 10\ \mu m$, $l = 70\ \mu m$, $\phi_0 = 90^0$, $\tau = 1$ ps, $T = 300$ K. (a) $\mu_c = 0$ eV; (b) $\mu_c = 0.1$ eV; (c) $\mu_c = 0.3$ eV; (d) $\mu_c = 0.5$ eV.

To demonstrate the features of the field behavior we calculated total magnetic field distribution near the plasmon resonance and the Rayleigh anomaly frequency. Figure 8 is plotted for the infinite periodic grating near the first plasmon resonance frequency, $f = 2.88$ THz, and near the Rayleigh anomaly frequency $f = 4.285$ THz,

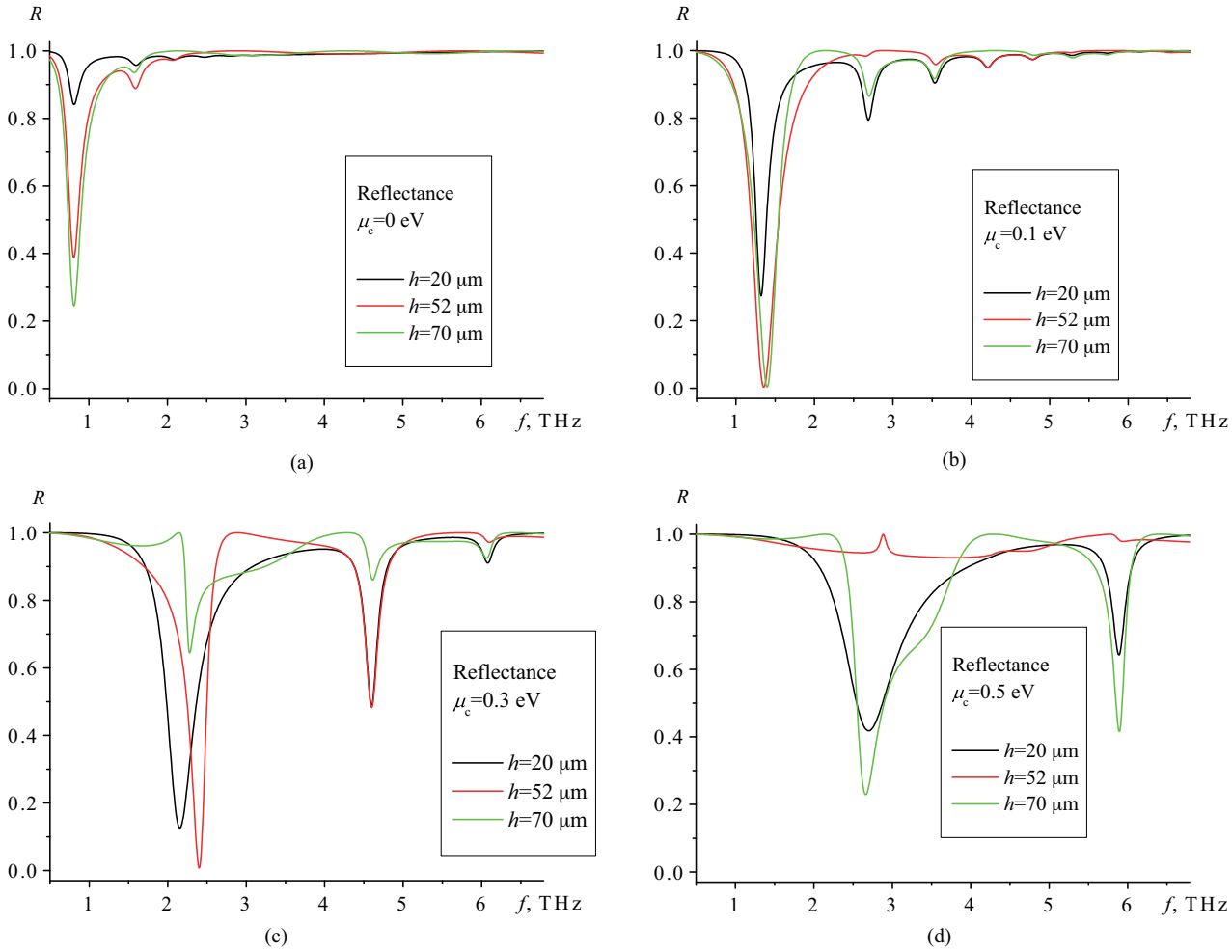

Figure 7. Dependences of reflection vs. frequency for infinite gratings above the PEC plane, $h = 20\ \mu m$ (black curves), $h = 52\ \mu m$ (red curves), $h = 70\ \mu m$ (green curves), $d = 10\ \mu m$, $l = 70\ \mu m$, $\phi_0 = 90^0$, $\tau = 1$ ps, $T = 300$ K. a) $\mu_c = 0$ eV; b) $\mu_c = 0.1$ eV; (c) $\mu_c = 0.3$ eV; (d) $\mu_c = 0.5$ eV.

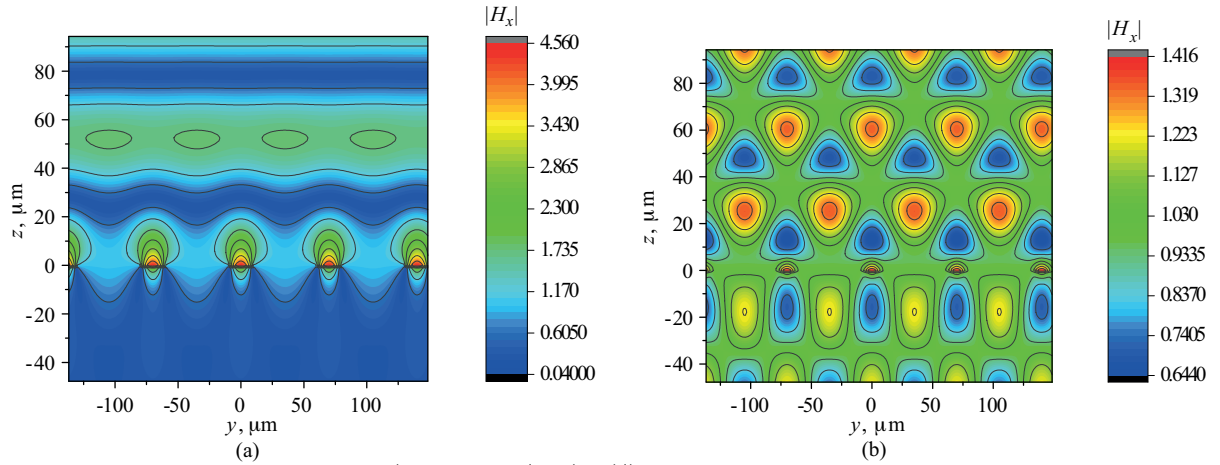

Figure 8. Total near field distribution (component $|H_x(y,z)|$) for the infinite periodic grating, $d = 10\ \mu m$, $l = 70\ \mu m$, $\phi_0 = 90^0$, $\tau = 1$ ps, $T = 300$ K, $\mu_c = 0.5$ eV, near a) the plasmon resonance, $f = 2.88$ THz, and b) the Rayleigh anomaly, $f = 4.85$ THz.

$\mu_c = 0.5$ eV. Figure 9 is plotted for the infinite periodic grating above the PEC plane near the first plasmon resonance for $f = 2.88$ THz and for two values of $h = 52\ \mu m$ and $h = 2d = 20\ \mu m$. Value $h = 52\ \mu m$ corresponds to the grating-plane resonance case when $R \approx 1$.

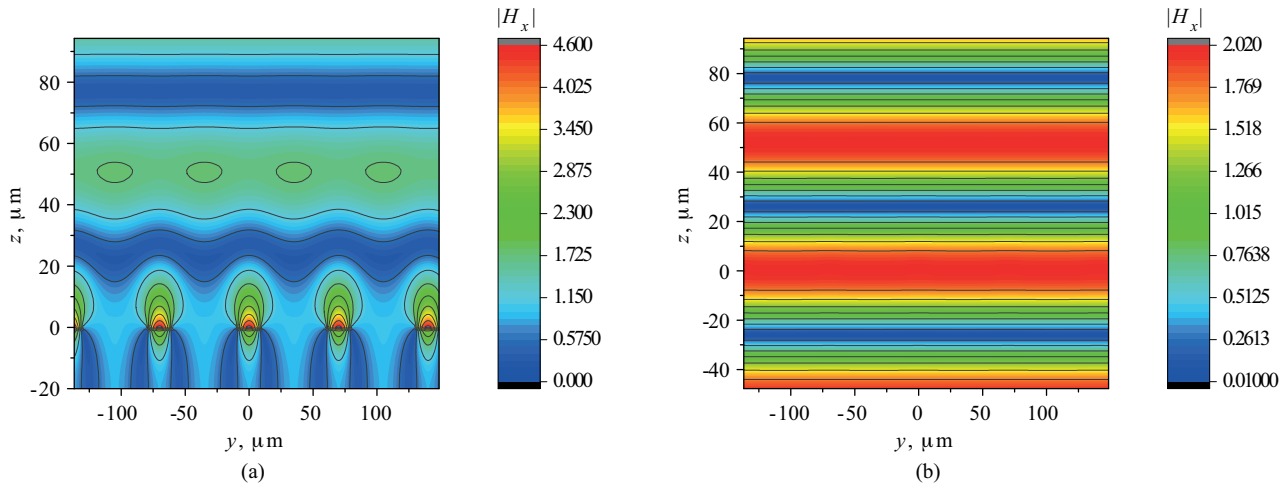

Figure 9. Total near field distribution (component $|H_x(y,z)|$) for the infinite periodic grating above the PEC plane near the plasmon resonance, $f = 2.88$ THz, $d = 10\ \mu m$, $l = 70\,\mu m$, $\phi_0 = 90^0$, $\tau = 1$ ps, $T = 300$ K, $\mu_c = 0.5$ eV, a) $h = 20\ \mu m$, b) $h = 52\ \mu m$.

6. Conclusions

In this paper, a rigorous solution of diffraction by the infinite periodic graphene grating and graphene grating above a PEC is obtained. The results of comparison with finite grating and of comparison with results obtained from scalar equations for the case when only one dominant plane wave may propagate are presented for validation.

We studied the scattering and absorption characteristics for different values of chemical potential and distance between the grating and the plane. Variety of surface plasmon resonances in the THz range was demonstrated. In the presence of the PEC plane the grating-plane resonances appear. Here one can observe almost total reflection without absorbance, even near the plasmon resonance frequencies.

References

[1] Kaliberda ME, Lytvynenko LM, Pogarsky SA. Modeling of graphene planar grating in the THz range by the method of singular integral equations. Frequenz 2017; 72: 277-284.

[2] Otsuji T, Tombet SAB, Satou A, Fukidome H, Suemitsu M, Sano E, Popov V, Ryzhii M, Ryzhii V. Graphene-based devices in terahertz science and technology. J Phys D Appl Phys 2012; 45: 303001.

[3] Avouris P. Graphene: electronic and photonic properties and devices. Nano Lett 2010; 10: 4285-4294.

[4] Islam MS, Kouzani AZ. Numerical investigation of a grating and graphene-based multilayer surface plasmon resonance biosensor. J Mod Optic 2014; 61: 1209-1218.

[5] Shapoval OV, Nosich AI. Bulk refractive-index sensitivities of the THz-range plasmon resonances on a micro-size graphene strip, J Phys D Appl Phys 2016; 49: 055105.

[6] Llatser I, Kremers C, Cabellos-Aparicio A, Jornet JM, Alarcon E, Chigrin DN. Graphene-based nano-patch antenna for terahertz radiation. Photonics Nanostruct 2012; 10: 353-358.

[7] Shao Y, Yang JJ, Huang M. A review of computational electromagnetic methods for graphene modeling. Int J Antenn Propag 2016; 2016: 7478621.

[8] Balaban MV, Shapoval OV, Nosich AI. THz wave scattering by a graphene strip and a disk in the free space: integral equation analysis and surface plasmon resonances. J Optics 2013; 15: 1-9.

[9] Shapoval OV, Gomez-Diaz JS, Perruisseau-Carrier J, Mosig JR, Nosich AI. Integral equation analysis of plane wave scattering by coplanar graphene-strip gratings in the THz range. IEEE T Terahertz Sci Technol 2013; 3: 666-674.

[10] Nikitin AY, Guinea F, Garcia-Vidal FJ, Martin-Moreno L. Edge and waveguide terahertz surface plasmon modes in graphene microribbons. Phys Rev B 2012; 85: 081405.

[11] Khavasi A. Fast convergent Fourier modal method for the analysis of periodic arrays of graphene ribbons. Opt Lett 2013; 38: 3009-3012.

[12] Zinenko TL. Scattering and absorption of terahertz waves by a free-standing infinite grating of graphene strips: analytical regularization analysis. J Optics 2015; 17: 1-8.

[13] Zinenko TL, Matsushima A, Nosich AI. Surface-plasmon, grating-mode, and slab-mode resonances in the H- and E-polarized THz wave scattering by a graphene strip grating embedded into a dielectric slab. IEEE J Sel Top Quantum Elect 2017; 23: 4601809.

[14] Shestopalov VP, Lytvynenko LM, Masalov SA, Sologub VG. Wave Diffraction by Gratings. Kharkiv, Ukraine: Kharkiv State University Press, 1973 (in Russian).

[15] Shestopalov VP. Summation Equations in the Modern Theory of Diffraction. Kyiv, Ukraine: Naukova Dumka, 1983 (in Russian).

[16] Shestopalov VP, Sirenko YK. Dynamical Theory of Gratings. Kyiv, Ukraine: Naukova Dumka, 1989 (in Russian).

[17] Lifanov IK. Singular Integral Equations and Discrete Vortices. Utrecht, the Netherlands: VSP, 1996.

[18] Gandel YV. Boundary-value problems for the Helmholtz equation and their discrete mathematical models. J Math Sci 2010; 171: 74-88.

[19] Nosich AA, Gandel YV. Numerical analysis of quasioptical multireflector antennas in 2-D with the method of discrete singularities: E-wave case. IEEE T Antenn Propag 2007; 55: 399-406.

[20] Gandel YV. Method of discrete singularities in electromagnetic problems. Problems of Cybernetics 1986; 124: 166-183 (in Russian with an abstract in English).

[21] Kaliberda ME, Lytvtnenko LM, Pogarsky SA. Singular integral equations in diffraction problem by an infinite periodic strip grating with one strip removed. J Electromagnet Wave 2016; 30: 2411-2426.

[22] Kaliberda M, Lytvynenko L, Pogarsky S. Method of singular integral equations in diffraction by semi-infnite grating: H -polarization case. Turk J Electr Eng & Comp Sci 2017; 25: 4496-4509.

[23] Hanson GW. Dyadic Green's functions and guided surface waves for a surface conductivity model of graphene. J Appl Phys 2008; 103: 064302.

[24] Hanson GW. Dyadic Green's functions for an anisotropic, non-local model of biased graphene. IEEE T Antenn Propag 2008; 56: 747-757.

[25] Fuscaldo W, Burghignoli P, Baccarelli P, Galli A. Ef?cient 2-D leaky-wave antenna con?gurations based on graphene metasurfaces. Int J Microw Wirel T 2017; 9: 1-11.

[26] Depine RA. Graphene Optics: Electromagnetic Solution of Canonical Problems. San Rafael, CA, USA: Morgan & Claypool Publishers, 2016.

[27] Warshawskaya NA, Gandel YV. Diffraction of a plane monochromatic wave on pre-Cantor gratings. Electromagnitnye Yavleniya 1998; 1: 455-464 (in Russian with an abstract in English).

[28] Gandel YV, Lifanov IK, Polanskaya TS. K obosnovaniyu vetoda diskretnyh osobennostej v dvumernyh zadachah difrakchii. Differential Equations 1995; 31: 1536-1541 (in Russian).